第27卷 第7期
2006年7月

半 导 体 学 报
CHINESE JOURNAL OF SEMICONDUCTORS

Vol. 27 No. 7
July, 2006

An Analytical Model for the Surface Electrical Field Distribution and Optimization of Bulk-Silicon Double RESURF Devices

Li Qi†, Li Zhaoji, and Zhang Bo

(*IC Design Center, University of Electronic Science and Technology of China, Chengdu 610054, China*)

Abstract: A new 2D analytical model for the surface electrical field distribution and optimization of bulk-silicon double RESURF devices is presented. Based on the solution to the 2D Poisson's equation, the model gives the influence on the surface electrical field of the drain bias and structure parameters such as the doping concentration, the depth and the position of the p-top region, the thickness and the doping concentration of the drift region, and the substrate doping concentration. The dependence of breakdown voltage on the length and doping concentration of the drift region is also calculated. Further more, an effective way to gain the optimum high-voltage is also proposed. All analytical results are verified by simulation results obtained by MEDICI and previous experimental data, showing the validity of the model presented here.

Key words: bulk-silicon; double RESURF; surface electrical field; optimization
EEACC: 2560B; 2560P
CLC number: TN432 **Document code:** A **Article ID:** 0253-4177(2006)07-1177-06

1 Introduction

In recent years, (reduced surface field RESURF) technology has been widely used in power integrated circuits device[1,2]. Double RESURF is one of the most widely used methods to design high voltage devices with low on-resistance. Much research by numerical simulation and experiment shows that high breakdown voltage can be maintained while the drift region doping concentration is increased to twice as much as that in single RESURF devices[3~7], and a good trade-off between breakdown voltage and on-resistance is realized. Several analytical models have previously been introduced[8~11] but are all for particular structures, providing little information about breakdown phenomena of bulk-silicon double RESURF devices. A simple method for determining the optimal charge balance and processing window of double RESURF lateral devices is presented by solving the 1D Poisson equation, because of the 2D nature of the charge distribution in the drift region, which cannot provide any detailed physical insight into the RESURF principles and device characteristics[7]. To the best of our knowledge, there has not been any 2D bulk-silicon analytical solution for the surface electrical field of double RESURF structure so far.

The purpose of this work is to develop a 2D analytical model for the surface electrical field and potential distributions of bulk-silicon double RESURF devices using the Poisson solution. The analytical results of the presented models show a good agreement with the numerical simulation results obtained by MEDICI and previous experimental data. The dependence of the surface electrical field on the bias and structure parameters has been discussed in detail. The proposed models will be helpful for designers to provide accurate first-order design schemes and afford an effective way to improve the performance of high voltage bulk-silicon double RESURF devices.

2 Analytical model

A schematic cross-section of the bulk-silicon double RESURF device is shown in Fig. 1, where x measures the horizontal position relative to the left edge of the double-diffused p^+n junction and y measures the vertical position relative to the surface. The drift region length is defined as the n^- type region length, $L_3 - L_0 = L_3$, between the n^+ drain and p^+ well. The drift region thickness is t_e, with a uniform doping concentration of N_e, where-

† Corresponding author. Email: lqphoenix@sina.com
Received 22 December 2005

as P_{top} and t_{top} are the doping concentration and depth of the p-top region, respectively. A negative

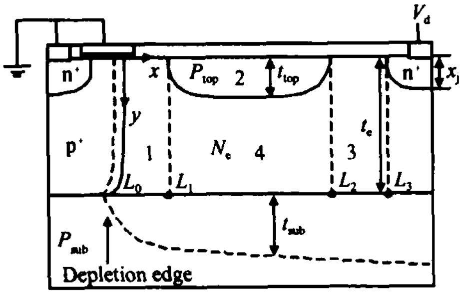

Fig. 1 Cross-section of the double RESURF device

concentration denotes p-type doping, and a positive concentration is n-type doping. The whole drift region is divided into four regions along the edges of the p-top region, and their boundary positions are given by $x = 0, L_1, L_2, L_3$ and $y = 0, t_{top}, t_e$. The substrate depletion layer thickness is t_{sub}, with doping concentration P_{sub}. The dielectric constant of bulk-silicon is ε_{si}. The device is biased in the off-state configuration; substrate, source, and gate are grounded while the drain is biased to a positive voltage V_d. The potential function $\phi_i(x, y)$ in the silicon film must satisfy the 2D Poisson's equation given by

$$\frac{\partial^2 \phi_i(x,y)}{\partial x^2} + \frac{\partial^2 \phi_i(x,y)}{\partial y^2} = -\frac{qN_i}{\varepsilon_{si}}, \quad i = 1,2,3,4 \tag{1}$$

Assuming that the drift region is completely depleted and the potential functions $\phi_i(x, y)$ can be approximated by the second order Taylor expansions

$$\phi_i(x,y) = \phi_i(x,0) + \frac{\partial \phi_i(x,0)}{\partial x} y + \frac{\partial^2 \phi_i(x,0)}{2\partial x^2} y^2, \quad i = 1,2,3 \tag{2}$$

$$\phi_4(x,y) = \phi_4(x,t_{top}) + \frac{\partial \phi_4(x,t_{top})}{\partial x}(y - t_{top}) + \frac{\partial \phi_4(x,t_{top})}{2\partial x^2}(y - t_{top})^2 \tag{3}$$

the boundary conditions for the potential functions are then

$$\left.\frac{\partial \phi_i(x,y)}{\partial y}\right|_{y=0} = 0, \quad i = 1,2,3 \tag{4}$$

$$\left.\frac{\partial \phi_i(x,y)}{\partial y}\right|_{y=t_e} = -\frac{2\phi_i(x,t_e)}{t_{sub}}, \quad i = 1,3,4 \tag{5}$$

$$\phi_2(x,t_{top}) = \phi_4(x,t_{top}), \quad \left.\frac{\partial \phi_2(x,y)}{\partial y}\right|_{y=t_{top}} = \left.\frac{\partial \phi_4(x,y)}{\partial y}\right|_{y=t_{top}} \tag{6}$$

$$\phi_1(L_1,0) = \phi_2(L_1,0), \quad \left.\frac{\partial \phi_1(L_1,y)}{\partial x}\right|_{y=0} = \left.\frac{\partial \phi_2(L_1,y)}{\partial x}\right|_{y=0} \tag{7}$$

$$\phi_2(L_2,0) = \phi_3(L_2,0), \quad \left.\frac{\partial \phi_2(L_2,y)}{\partial x}\right|_{y=0} = \left.\frac{\partial \phi_3(L_2,y)}{\partial x}\right|_{y=0} \tag{8}$$

$$\phi_1(0,0) = 0, \quad \phi_3(L_3,0) = V_d \tag{9}$$

where $N_1 = N_3 = N_4 = N_e$, $N_2 = P_{top}$. Equation (4) assumes that the electric field at the surface can be minimized[12]. Equation (5) is obtained from a linear field variation along the vertical direction within the substrate depletion thickness t_{sub}. Equations (6)～(8) are the continuity of the potential and electrical field along the boundary of regions 1-2, 2-3, and 2-4, respectively, and Equation (9) is the voltage condition applied to the device. Substituting Eqs. (2) and (3) into Eq. (1) under boundary conditions Eqs. (4)～(6) leads to a general differential equation for the potential distribution function along the surface:

$$\frac{\partial^2 \phi_i(x,0)}{\partial x^2} + \frac{\phi_i(x,0)}{t^2} = -\frac{qN_{eff}^i}{\varepsilon_s}, \quad i = 1,2,3 \tag{10}$$

Here $N_{eff}^1 = N_{eff}^3 = N_e$, $t = \sqrt{\frac{t_e^2 + t_e t_{sub}}{2}}$ and $N_{eff}^2 = -P_{top} + \frac{P_{top} + N_e}{t_e^2 + t_e t_{sub}}((t_e - t_{top})^2 + t_{sub}(t_e - t_{top}))$.

We assume that t_{sub} is a constant in the first-order approximation, and with the general formula for the double-sided junction may be taken as

$$t_{sub} = \frac{1}{2} \times \left(\sqrt{\left(1 + \frac{N_{eff}^3}{P_{sub}}\right) t_e^2 + \frac{2\varepsilon_s V_d}{qP_{sub}}} - t_e\right)$$

Solving Eq. (10) with the boundary conditions $\phi_1(L_1,0) = V_1$, $\phi_2(L_2,0) = V_2$ and $\phi_3(L_3,0) = V_3$ gives the surface potential $\phi_i(x,0)$ and electrical field $E_i(x,0)$ as

$$\phi_i(x,0) = \frac{qN_{eff}^i t^2}{\varepsilon_s} + \left(V_i - \frac{qN_{eff}^i t^2}{\varepsilon_s}\right) \times \frac{\sinh((x - L_{i-1})/t)}{\sinh((L_i - L_{i-1})/t)} + \left(V_{i-1} - \frac{qN_{eff}^i t^2}{\varepsilon_s}\right) \times \frac{\sinh((L_i - x)/t)}{\sinh((L_i - L_{i-1})/t)}, \quad L_{i-1} \leq x < L_i \tag{11}$$

$$E_i(x,0) = \left(V_i - \frac{qN_{eff}^i t^2}{\varepsilon_s}\right) \times \frac{\cosh((x - L_{i-1})/t)}{t\sinh((L_i - L_{i-1})/t)} - \left(V_{i-1} - \frac{qN_{eff}^i t^2}{\varepsilon_s}\right) \times \frac{\cosh((L_i - x)/t)}{t\sinh((L_i - L_{i-1})/t)}, \quad L_{i-1} \leq x < L_i \tag{12}$$

where $i = 1, 2$, and 3 are applied, V_1 and V_2 are the surface potential of two boundaries between the p-top and drift regions, respectively. The surface potential $\phi_i(x, 0)$ and surface electrical field $E_i(x, 0)$ are now obtained from Eqs. (11) and (12), respectively, by finding V_1 and V_2 for given $V_0 = 0$ and $V_3 = V_d$ using the continuity condition Eqs. (8) and (9). Using $P_{top} = N_e$ in Eq. (12), the surface electric field of a single RESURF device can be obtained by

$$E(x,0) = \left(V_d - \frac{qN_e t^2}{\varepsilon_s}\right) \times \frac{\cosh(x/t)}{t\sinh(L_3/t)} + \frac{qN_e t}{\varepsilon_s} \times \frac{\cosh((L_3 - x)/t)}{\sinh(L_3/t)}, \quad 0 \leq x < L_3 \tag{13}$$

3 Results and discussion

In order to verify the proposed model, a 2D device simulation is performed using MEDICI for the same structure. In the following figures, the curves denote the analytical results and the points represent the numerical results.

Figure 2 shows the surface potential and electrical field distributions of single RESURF and double RESURF devices. A fair accordance between the analytical and numerical results may generally be found. The discrepancies between them are due to the penetration of the space charge region between two regions with different doping concentrations in $x = 0, L_1, L_2$ and L_3. However, this kind of discrepancy has little effect on the breakdown voltage analysis. One can see that a new electric field peak appears at $x = L_2$ in the double RESURF device as compared to the single RESURF structure. Because of the incorporation of the p-top region inside the drift region, the peaks of the electric field of the double RESURF is decreased at $x = 0$ and increased a little at $x = L_3$. The potential of the double RESURF is distributed linearly in most of the drift region, but the potential distribution of the single RESURF shows a large curvature in the whole drift region, which leads to a non-uniform surface field profile that may cause the degradation of the breakdown voltage.

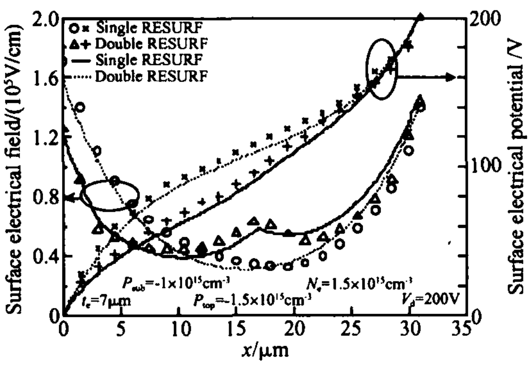

Fig. 2　Surface potential and electrical field distributions of single RESURF and double RESURF devices

Figure 3 illustrates the surface electrical distributions for different doping concentrations, thicknesses, and positions of the p-top region. It is

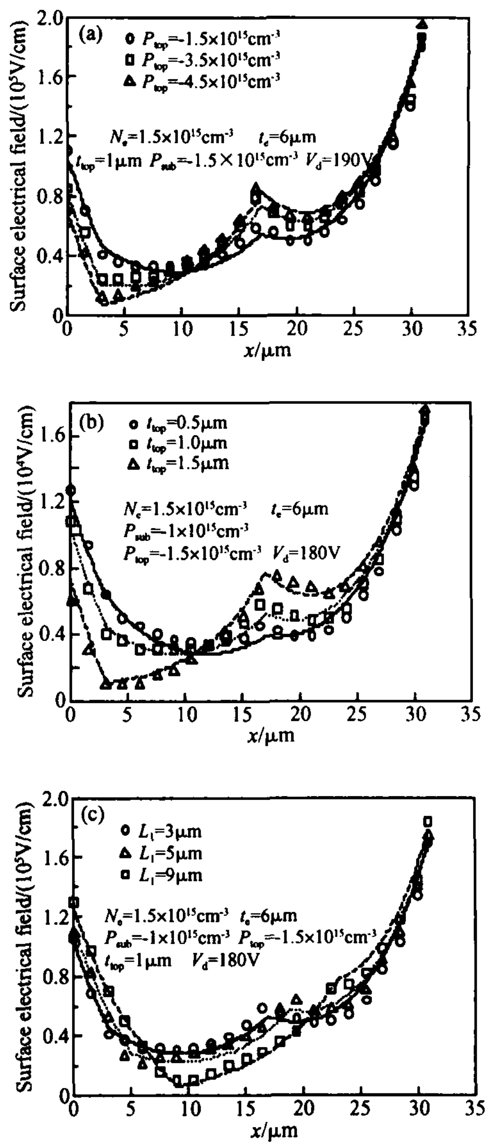

Fig. 3　Surface electrical distributions of the double RESURF device along the drift region　(a) Different P_{top}; (b) Different t_{top}; (c) Different L_1

evident that there are three surface electric field peaks, which appear at $x = 0$, L_2 and L_3, respectively, and strongly depend on the parameters of the p-top region. In Fig. 3(a) and (b), P_{top} and t_{top} have the same effect on the surface electric field distribution. With an increase in P_{top} or t_{top}, the electric field peaks decrease at $x = 0$ and increase at $x = L_2$, L_3, and there exists an electric field value that is fixed between $x = L_1$ and L_2. This means that the highest electric field may move from $x = L_3$ to $x = 0$ with a decrease in P_{top} or t_{top}, which is responsible for the change of the potential distribution. Therefore the breakdown point moves from $x = L_3$ to $x = 0$ as P_{top} or t_{top} decreases below a critical value, at which the two electric field peaks ($x = 0$, L_3) are equal. In Fig. 3(c), the position of the electric field peaks at $x = L_2$ moves with the change of the p-top region position, while the positions of other electric field peaks do not change. Because the p-top region's charge can restrain the peaks at $x = 0$, but enhance those at other places, one can find that with the increase of L_1, the values of the electric field at $x = 0$, L_2, and L_3 increase, but the value of the electric field decreases at $x = L_1$. Therefore, in order to obtain the ideal electric field distribution at which the maximum breakdown is realized, a smaller L_1 is required.

Figure 4 demonstrates the surface electric field distributions for different drift region doping concentrations, thicknesses, and substrate doping concentrations. In Figs. 4(a) and (b), with the increase of N_e or t_e, the magnitude of the electric field increases at $x = 0$, L_1, and decreases at $x = L_3$, but is fixed at $x = L_2$, so the maximum peak field point may translate from $x = L_3$ to $x = 0$. The maximum breakdown point will change with a change of the position of the highest electric field peak value. When the three electric field peaks ($x = 0$, L_2, L_3) have a uniform value, which must be less than the critical value, the maximum breakdown voltage will appear. In contrast, the substrate doping concentration of the substrate causes the magnitude of the peak field to decrease at $x = 0$ and increase at $x = L_3$ with the increase in the substrate doping concentration. In the optimization of the devices, the substrate doping concentration is a very important parameter, which to a large extent determines the position and amplitude of the maximum peak electric field.

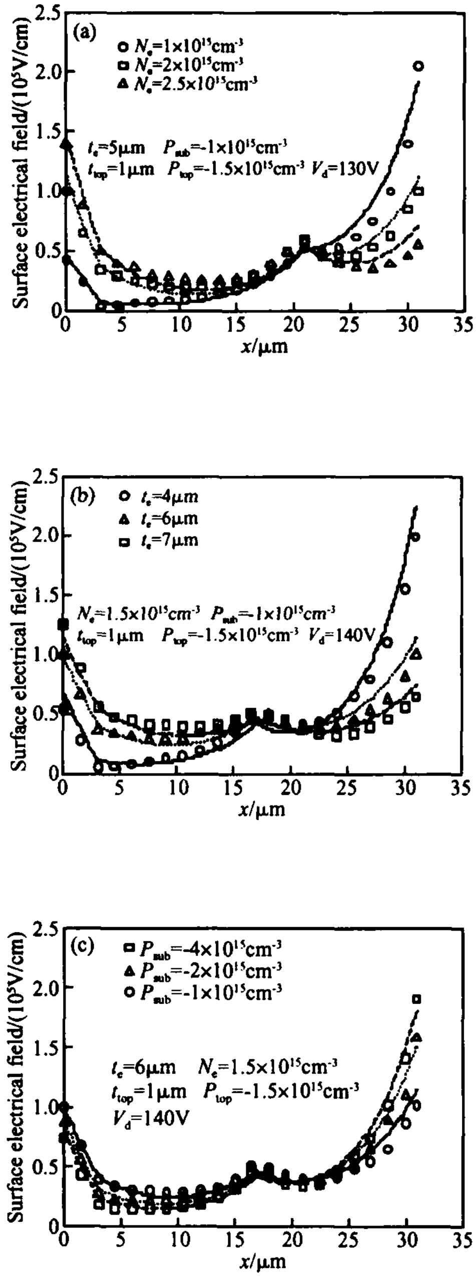

Fig. 4 Surface electrical distributions of double RESURF device along the drift region (a) For different drift region doping concentrations; (b) For different drift region thicknesses; (c) For different substrate doping concentrations

The breakdown voltage of a double RESURF device is determined by the minimum of the lateral breakdown voltage BV_{lat}, and the vertical breakdown voltage BV_{ver}. BV_{lat} due to the surface electric field $E_i(x,0)$ can be calculated from the avalanche breakdown condition of the critical electric field concept. The maximum surface electric field reaches the critical value E_{clat}, which can be given as

$$\mathrm{Max}[E_i(x,0)] = E_{clat} = \frac{A}{1 - B\lg\frac{N_e}{10^{16}}}$$

where $A \cong 3.1\mathrm{V/cm}$ and $B \cong 0.5$ are related to the ionization rates[13]. BV_{ver} is determined solving the ionization integral with ionization rates for an abrupt two-sided p-n junction[14]:

$$BV_{ver} = 5.238 \times 10^{13} \times \left(\frac{P_{sub}}{1+\frac{P_{sub}}{N_e}}\right)^{-\frac{3}{4}} \left[1 - \frac{\left(1-\frac{t_e N_e}{T_y P_{sub}}\right)^2}{1+\frac{N_e}{P_{sub}}}\right]$$

with $T_y \approx \left[\frac{1.8\times 10^{-35}}{8} \times \left(\frac{qP_{sub}}{\varepsilon_s}\right)^7 \times \left(1+\frac{P_{sub}}{N_e}\right)\right]^{-\frac{1}{8}}$.

Analytical results for the breakdown voltage are shown in Fig. 5 with simulation results as a function of the drift region length for a set of device parameters and compared with the experimental data obtained by Colak[15]. One can see that both show good accordance. For a given set of parameters, with the increase of the drift region length, the breakdown voltage reaches a constant value BV_{ver} that is limited by the vertical p-n junction breakdown.

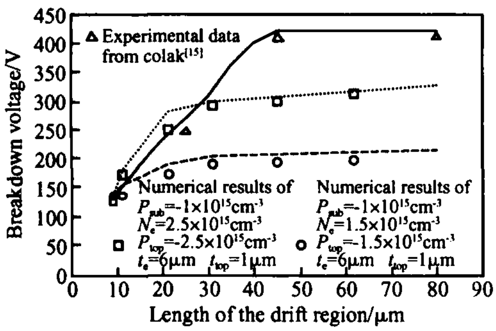

Fig. 5　Breakdown voltage as a function of drift region length

Figure 6 gives the critical drift region thickness and breakdown voltage change as a function of drift region doping concentration. There exists an optical drift region doping concentration at which the maximum breakdown voltage occurs for a double RESURF, which is similar to the results given by Souza[3]. For a certain drift region thickness, a double RESURF device allows a significant increase in the drift region doping concentration responsible for the reduction of the on-resistance when compared with a single RESURF device, which improves the trade-off between the breakdown voltage and on-resistance.

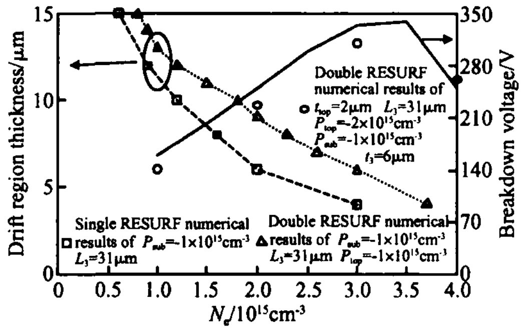

Fig. 6　Critical drift region thickness and breakdown voltage as a function of drift region doping concentration

4　Conclusion

The surface field distribution and optimal design of double RESURF devices have been studied analytically. The dependence of the surface electric field and potential distributions on the thickness and doping concentration of the drift region, depth, doping concentration, and position of the p-top region and substrate doping concentration and the influence of the drift region length and doping concentration on the breakdown voltage also have been discussed. All analytical results have been shown to be in agreement with the results obtained by the MEDICI simulation. In order to enhance the breakdown characteristics of the devices while maintaining the low on-resistance, an ideal surface field distribution is much needed and the critical doping concentration of P_{top} and N_e is of considerable importance. Therefore, the analytical model proposed in this paper will be a good tool for a designer to optimize double RESURF devices.

References

[1] Appels J, Vaes H, Verhoeven J. High voltage thin layer devices (RESURF devices). IEDM Tech Digest, 1979: 238
[2] Baliga B J. An overview of smart power technology. IEEE Trans Electron Devices, 1991, 38(7): 1568
[3] Souza M M D, Narayanan E M S. Double RESURF technology for HVIC. Electron Lett, 1996, 32 (12): 1092
[4] Hardikar S, de Souza M M, Xu Y Z, et al. A novel double RESURF LDMOS for HVIC's. J Microelectron, 2004, 35(35): 305
[5] Parthasarathy V, Khemka V, Zhu R, et al. SOA improvement by a double RESURF LDMOS technique in a power IC technology. IEDM, 2000: 75
[6] Hossain Z, Imam M, Fulton J, et al. Double-RESUF 720V n-channel LDMOS with best-in-class on-resistance. Proceedings of ISPSD, 2002: 137

[7] Imam M, Hossain Z, Quddus M, et al. Design and optimization of double-RESURF high-voltage lateral devices for a manufacturable process. IEEE Trans Electron Devices, 2003, 20 (7): 1697

[8] Fang Jian, Yi Kun, Li Zhaoji, et al. On-state breakdown model for high voltage RESURF LDMOS. Chinese Journal of Semiconductors, 2005, 26(3): 436

[9] Li Qi, Zhang Bo, Li Zhaoji. A breakdown model of thin drift region LDMOS with a step doping profile. Chinese Journal of Semiconductors, 2005, 26(11): 120 (in Chinese) [李琦, 张波, 李肇基. 阶梯掺杂薄漂移区 RESURF LDMOS 耐压模型. 半导体学报, 2005, 26(11): 120]

[10] Guo Yufeng, Zhang Bo, Mao Ping, et al. Unified breakdown model of SOI RESURF device with uniform/step/linear doping profile. Chinese Journal of Semiconductors, 2005, 26(2): 243

[11] Imam M, Quddus M, Adams J, et al. Efficacy of charge sharing in reshaping the surface electric field in high-voltage lateral RESURF Devices. IEEE Trans Electron Devices, 2004, 51: 141

[12] Han S Y, Kim H W, Chung S K. Surface field distribution and breakdown voltage of RESURF LDMOSFETs. J Microelectron, 2000, 31: 685

[13] Sze S M. Physics of semiconductor devices. New York: Wiley, 1981

[14] Han S Y, Na J M, Choi Y I, et al. An analytical model of the breakdown voltage and minimum EPI layer length for RESURF pn diodes. Solid-State Electron, 1996, 39(8): 1353

[15] Colak S. Effects of drift region parameters on the static properties of power LDMOST. IEEE Trans Electron Devices, 1981, 28(12): 1455

体硅 Double RESURF 器件表面电场解析模型及优化设计

李 琦[†] 李肇基 张 波

(电子科技大学 IC 设计中心, 成都 610054)

摘要: 提出了体硅 double RESURF 器件的表面电场和电势的解析模型. 基于分区求解二维 Poisson 方程, 获得 double RESURF 表面电场的解析表达式. 借助此模型, 研究了 p-top 区的结深, 掺杂浓度和位置, 漂移区的厚度和掺杂浓度, 及衬底浓度对表面电场的影响; 计算了漂移区长度, 掺杂浓度和击穿电压的关系. 从理论上揭示了获得最大击穿电压的条件. 解析结果、验证结果和数值结果吻合良好.

关键词: 体硅; double RESURF; 表面电场; 优化设计

EEACC: 2560B; 2560P

中图分类号: TN432 **文献标识码**: A **文章编号**: 0253-4177(2006)07-1177-06

† 通信作者. Email: lqphoenix@sina.com

2005-12-22 收到